INFECTION AND IMMUNITY, Dec. 2004, p. 6826–6835 Vol. 72, No. 12
0019-9567/04/$08.00+0 DOI: 10.1128/IAI.72.12.6826–6835.2004

Vesicular Transport Is Not Required for the Cytoplasmic Pool of Cholera Toxin To Interact with the Stimulatory Alpha Subunit of the Heterotrimeric G Protein

Ken Teter,† Michael G. Jobling, and Randall K. Holmes*

Department of Microbiology, University of Colorado Health Sciences Center, Denver, Colorado

Received 2 April 2004/Returned for modification 13 May 2004/Accepted 12 August 2004

Cholera toxin (CT) moves from the cell surface to the endoplasmic reticulum (ER) by retrograde vesicular transport. The catalytic A1 polypeptide of CT (CTA1) then crosses the ER membrane, enters the cytosol, ADP-ribosylates the stimulatory α subunit of the heterotrimeric G protein (Gsα) at the cytoplasmic face of the plasma membrane, and activates adenylate cyclase. The cytosolic pool of CTA1 may reach the plasma membrane and its Gsα target by traveling on anterograde-directed transport vesicles. We examined this possibility with the use of a plasmid-based transfection system that directed newly synthesized CTA1 to either the ER lumen or the cytosol of CHO cells. Such a system allowed us to bypass the CT retrograde trafficking itinerary from the cell surface to the ER. Previous work has shown that the ER-localized pool of CTA1 is rapidly exported from the ER to the cytosol. Expression of CTA1 in either the ER or the cytosol led to the activation of Gsα, and Gsα activation was not inhibited in transfected cells exposed to drugs that inhibit vesicular traffic. Thus, anterograde transport from the ER to the plasma membrane is not required for the cytotoxic action of CTA1.

Vibrio cholerae produces cholera toxin (CT), a protein that induces the life-threatening diarrhea characteristic of cholera. CT ADP-ribosylates and irreversibly activates the stimulatory α-subunit of the heterotrimeric G protein (Gsα) at the cytoplasmic face of the plasma membrane. Activated Gsα stimulates adenylate cyclase activity, and the subsequent increase in intracellular adenosine-3′,5′-monophosphate (cAMP) triggers chloride efflux from intoxicated intestinal epithelial cells. Diarrhea results from the osmotic movement of water that follows chloride efflux into the intestinal lumen (reviewed in reference 35).

CT is an AB_5-type protein toxin with a catalytic A subunit and a cell-binding B subunit (reviewed in reference 9). Proteolytic nicking of the A subunit at arginine 192 generates separate N-terminal A1 and C-terminal A2 fragments that remain linked by a disulfide bond between the cysteine residues at positions 187 and 199 in CTA. Catalytic activity resides in the CTA1 polypeptide, while the CTA2 polypeptide links CTA1 to CTB and stabilizes the holotoxin. The B subunit of CT is organized as a homopentameric ring-like structure that binds to GM1 gangliosides on the eukaryotic plasma membrane. Binding to GM1 gangliosides triggers toxin internalization from the cell surface through a caveolae or caveolae-like endocytic mechanism (1, 6, 30, 43). The active pool of internalized toxin subsequently moves from the endosomes to the Golgi and travels to the endoplasmic reticulum (ER) by retrograde vesicular transport (6, 15, 17, 22, 24, 26, 29). Reduction of the CTA1-CTA2 disulfide bond occurs in the ER, and a redox-dependent chaperone known as protein disulfide isomerase (PDI) catalyzes the release of CTA1 from CTA2/CTB_5 (28, 40). The released CTA1 polypeptide then crosses the ER membrane, enters the cytosol, and initiates the major toxic effects of CT.

Previous work has examined the trafficking of CT from the cell surface to the ER, the movement of CTA1 from the ER to the cytosol, and the interactions between CTA1 and Gsα (reviewed in references 19, 21, and 35). However, the mechanism by which the cytosolic pool of CTA1 reaches its Gsα target remains unknown. One possibility is that CTA1 simply diffuses through the cytosol to the plasma membrane, where Gsα is located. Another possibility is that CTA1 associates with the cytoplasmic face of the endomembrane system (either ER or Golgi membranes) after it enters the cytosol and travels on the cytoplasmic face of anterograde-directed transport vesicles in order to reach Gsα at the plasma membrane (9, 12, 19). Association with the ER or Golgi membrane could be facilitated by (i) direct insertion of the CTA1 polypeptide into the cytosolic leaflet of the ER membrane (7); (ii) interactions between CTA1 and a membrane-associated protein such as ARF1 (25); or (iii) continued tethering of CTA1 to the CT holotoxin via a membrane-spanning interaction with the lumenally oriented CTA2/CTB_5 portion of the toxin (16, 20). The possibility of a restricted cytosolic distribution for CTA1 (i.e., membrane association) was also inferred from the limited number of proteins ADP-ribosylated by CT in vivo compared to the larger number of proteins ADP-ribosylated by CT in vitro (42). Furthermore, a 15°C temperature block imposed 25 to 30 min after the addition of CT to cultures of T84 cells inhibited toxin activity but not the dissociation of CTA1 from CTA2/CTB_5 in the ER lumen (17, 18). Since vesicular transport from the ER to the Golgi is blocked at 15°C (32), this result suggested that

* Corresponding author. Mailing address: Department of Microbiology, Box B-175, University of Colorado Health Sciences Center, 4200 East Ninth Ave., Denver, CO 80262. Phone: (303) 315-7903. Fax: (303) 315-6785. E-mail: Randall.Holmes@UCHSC.edu.

† Present address: Biomolecular Science Center, Department of Molecular Biology and Microbiology, University of Central Florida, Orlando, FL 32826.

the pool of free CTA1 requires anterograde vesicular trafficking in order to access its Gsα target. The intoxication process would thus involve retrograde vesicular trafficking of CT from the plasma membrane to the ER and then anterograde trafficking of cytosolic CTA1 from the ER to the cytoplasmic face of the plasma membrane where Gsα resides. A similar trafficking pathway has also been discussed for pertussis toxin, an AB-type protein toxin that enters the cytosol after retrograde trafficking to the ER and ADP-ribosylates the inhibitory Gα at the cytoplasmic face of the plasma membrane (44, 45).

Technical limitations have made it difficult to evaluate directly the possible role of anterograde transport in the delivery of CTA1 from the ER to its target in intoxicated cells. Common methods for detecting CTA1 activity in the cytosol—elevated levels of intracellular cAMP, morphological changes to Y1 or CHO cultured cells, chloride efflux from polarized epithelial cells, and fluid accumulation in ileal loops—involve the addition of CT to the extracellular medium. With these methods, CT must undergo a series of retrograde vesicular trafficking events before the CTA1 polypeptide can cross the ER membrane and enter the cytosol. Disruptions to retrograde transport therefore inhibit the cellular response to exogenously added CT (15, 17, 22, 24, 26, 29). Unfortunately, disruptions to anterograde transport often have a corresponding inhibitory effect on retrograde transport. Any block of CTA1 anterograde transport could therefore inhibit CT retrograde transport as well. Experiments that use exogenously added CT to study CTA1 trafficking from the ER to the plasma membrane thus suffer from problems in reciprocity of anterograde-retrograde trafficking blocks.

Our investigators recently described a plasmid-based transfection system that allows direct delivery of newly synthesized CTA1 into the ER lumen of cultured cells (38). Biochemical methods demonstrated that the entire pool of newly synthesized CTA1 was cotranslationally inserted into the ER lumen (38). With this system, our group found that the ER-localized pool of CTA1 was rapidly exported from the ER to the cytosol and was degraded in the cytosol by a proteosome-dependent mechanism. However, our previous work was conducted with an enzymatically inactive CTA1 construct that contained aspartate-for-glutamate substitutions at residues 110 and 112 in the CTA1 active site and a C-terminal CVIM farnesylation consensus sequence. In this study we examined the consequences of delivering active forms of CTA1 into either the ER lumen or the cytosol of cultured CHO cells. CTA1 elicited a cAMP response from transfected cells when expressed in either the ER or the cytosol. Since this transfection-cAMP assay does not involve retrograde trafficking of CT from the cell surface to the ER, we were able to examine directly the putative role of anterograde vesicular transport in CTA1 activity. As disruption of anterograde transport did not alter the cellular response to CTA1 expression in either the ER or the cytosol, our results indicate that a functional secretory pathway is not required for the cytosolic pool of CTA1 to interact with its Gsα target.

MATERIALS AND METHODS

Materials. Chemicals, protein A-Sepharose, and protein G-agarose were purchased from Sigma-Aldrich (St. Louis, Mo.). Cell culture reagents were from Gibco BRL (Grand Island, N.Y.), while Lipofectamine was from Invitrogen (Carlsbad, Calif.). Monoclonal and polyclonal antibodies to CTA were produced in this lab (10, 11), the anti-α1-antitrypsin (α1AT) antibody was from DAKO (Carpinteria, Calif.), the anti-PDI antibody was from Stressgen (San Diego, Calif.), and the secondary antibodies were from Jackson ImmunoResearch Laboratories (West Grove, Pa.). Immobilized antibodies were generated by a 4°C overnight incubation with 50 mg of protein G-agarose (anti-CTA antibody) or 100 mg of protein A-Sepharose (anti-α1AT antibody) in 1 ml of phosphate-buffered saline supplemented with 0.1% bovine serum albumin. [^{35}S]methionine was purchased from NEN Life Sciences (Boston, Mass.). The [^{125}I]cAMP Biotrak competition assay kit was from Amersham-Pharmacia (Arlington Heights, Ill.). The Chinese hamster ovary (CHO) fibroblasts used in this study are auxotrophic for proline and were provided by Henry Wu (Uniformed Services University of the Health Sciences, Bethesda, Md.). A. A. McCracken (University of Nevada, Reno) kindly provided the pSV7/α1AT-M plasmid.

CTA1 expression constructs. The constructs used in this study are derivatives of pcDNA3.1/CTA1-CVIM, a previously described plasmid that uses a synthetic Kozak sequence in front of the native CTA signal sequence (denoted by ss) to drive the expression of a CTA1 variant with a C-terminal CVIM tag (38). The CVIM-tagged CTA1 variant was replaced with the native CTA1 sequence by cloning an XbaI-PstI fragment from a PCR product using a reverse primer (CCCTGCAGTCATTATCTTGGAGCATTCCCAC) that adds two stop codons and a PstI site (underlined) immediately after the arg-192 codon. Clones of wild-type or enzymatically inactive (E110D and E112D substitutions, denoted by dd) CTA variants were used as PCR templates to produce pcDNA3.1/ssCTA1 and pcDNA3.1/ddCTA1, respectively. pcDNA3.1/mCTA1 was generated in a similar manner: the E110D and E112D substitutions and CVIM tag in a ddCTA1-CVIM variant lacking the CTA signal sequence (39) were replaced with wild-type CTA1 sequences. All constructs were verified by DNA sequencing.

Cell culture and transfection. CHO cells were maintained in Ham's F-12 medium supplemented with 10% fetal bovine serum. Growth conditions were at 37°C and 5% CO_2 in a humidified incubator. For transient transfections, pcDNA3.1 expression plasmids (Invitrogen) containing our recombinant constructs were mixed with Lipofectamine as per the manufacturer's instructions. The mixtures were then added for 3 h to cells that had been seeded in six-well plates at 75% confluency 16 to 24 h before transfection. For immunofluorescence experiments, cells to be transfected were seeded at 25% confluency directly onto coverslips. Transfected cells were utilized at 2 to 4 h posttransfection (cAMP assays) or 24 h posttransfection (immunofluorescence and metabolic labeling).

Immunofluorescence. Transfected cells were fixed with a 20-min incubation in 3.7% formaldehyde and permeabilized with a 2-min incubation in ice-cold methanol. Monoclonal anti-CTA and rabbit polyclonal anti-PDI antibodies were then added for 1 h. After an additional 30-min incubation with fluorescein isothiocyanate-conjugated goat anti-mouse immunoglobulin G (IgG) and rhodamine-conjugated donkey anti-rabbit IgG antibodies, the intracellular distributions of CTA1 and PDI were visualized with a Nikon Eclipse TE200 microscope (Melville, N.Y.) and a 63× objective.

cAMP assay. Transfected cells were solubilized in 0.75 ml of acidic ethanol (1 N HCl–EtOH at a 1:100 ratio) for 15 min at 4°C. The supernatant was then collected after a 10-min 4°C spin, and a second extraction with 0.75 ml of an ice-cold ethanol-H_2O solution at a 2:11 ratio was performed on the remaining cell pellet. Supernatants from both extractions were combined and lyophilized overnight. cAMP levels in the lyophilized extracts were then quantitated with a [^{125}I]cAMP competition assay. Background cAMP levels from cells transfected with the empty pcDNA3.1 vector (typically 800 to 1,000 fmol of cAMP/well) were subtracted from the values obtained for our experimental conditions.

Metabolic labeling and immunoprecipitation. Cells transfected with a plasmid encoding the wild-type variant of α1-antitrypsin (α1AT-M) were bathed in methionine-free medium for 1 h, incubated with 0.5 ml of a 40-μCi/ml solution of [^{35}S]methionine for 30 min, and returned to serum-free medium containing 0.5 mg of methionine/ml for 0 or 90 min of chase. At min 0 of chase, cell extracts were generated by solubilization in 1 ml of lysis buffer (25 mM Tris [pH 7.4], 20 mM NaCl, 1% deoxycholic acid, 1% Triton X-100, 1 mM phenylmethylsulfonyl fluoride, 1 μg of pepstatin/ml, and 1 μg of leupeptin/ml) for 20 min at 4°C. Insoluble debris was subsequently removed by centrifugation. At 90 min of chase, the extracellular medium was collected and centrifuged to remove any cells that might have detached from the substratum. Both cell extracts and extracellular media were mixed with immobilized anti-α1AT antibodies for an overnight incubation. The bound material was then washed multiple times with 150 mM NaCl in NDET (1% NP-40, 0.4% deoxycholic acid, 5 mM EDTA, 10 mM Tris; pH 7.4) and resuspended in sample buffer. A PhosphorImager (Bio-Rad, Hercules, Calif.) was used to visualize and quantitate the immunoprecipitated pools of α1AT-M that were resolved by sodium dodecyl sulfate–9% polyacrylamide gel electrophoresis (SDS-PAGE). For quantitation, the secreted pools of α1AT-M

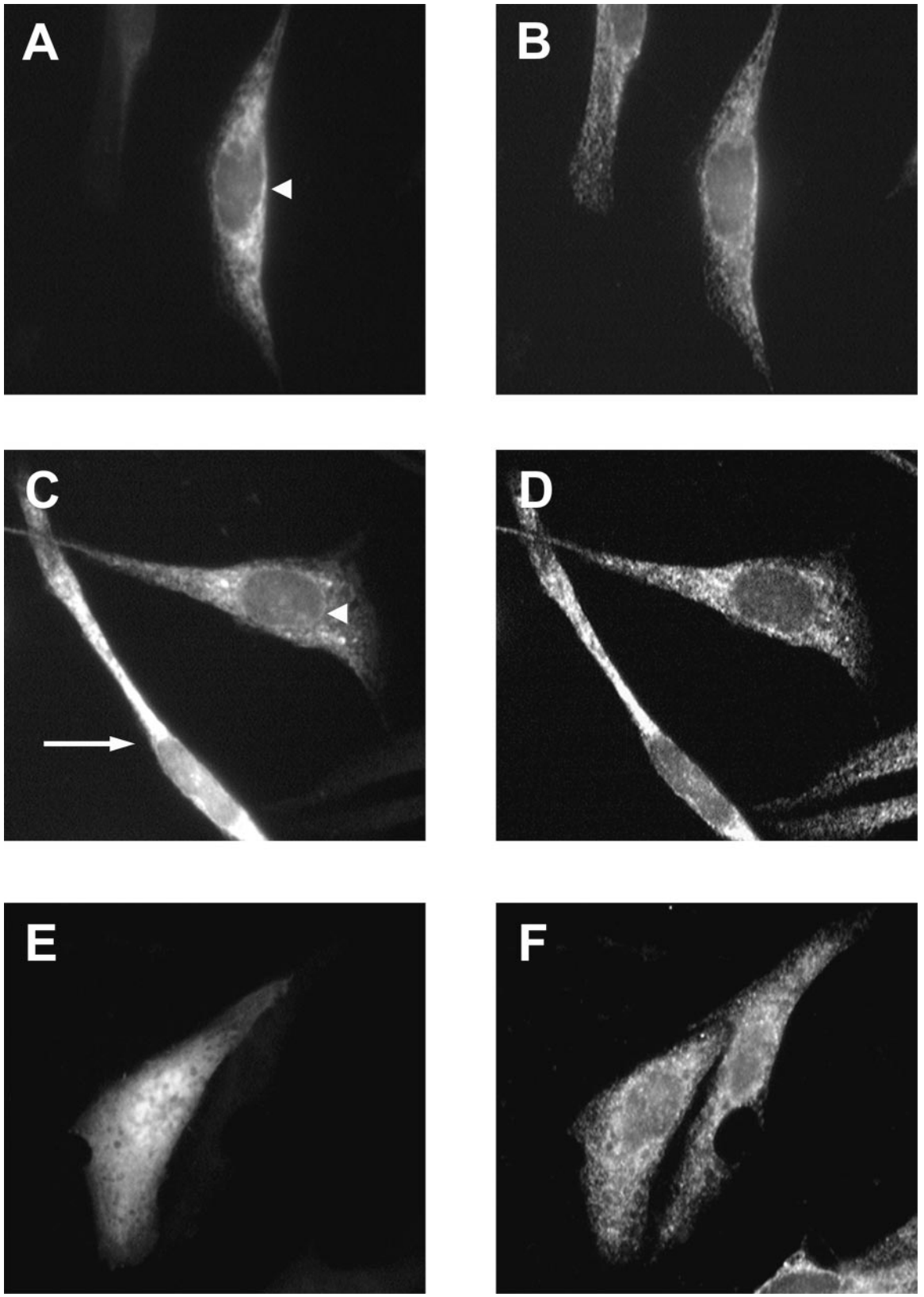

FIG. 1. Intracellular distribution of ddCTA1, ssCTA1, and mCTA1. CHO cells were transiently transfected with pcDNA3.1/ddCTA1 (A and B), pcDNA3.1/ssCTA1 (C and D), or pcDNA3.1/mCTA1 (E and F). At 24 h posttransfection the cells were fixed, permeabilized, and exposed to a mixture of mouse anti-CTA and rabbit anti-PDI antibodies for 1 h. The cells were then incubated with fluorescein isothiocyanate-conjugated goat anti-mouse IgG and rhodamine-conjugated donkey anti-rabbit IgG antibodies for 30 min. Expression patterns of the CTA1 constructs are shown in panels A, C, and E; the distribution of PDI, a resident ER enzyme, is shown in panels B, D, and F. Arrowheads in panels A and C denote CTA1 labeling of the nuclear envelope, which is physically contiguous with the ER. The arrow in panel C marks a cell with the elongated and bipolar morphology characteristic of CT-intoxicated CHO cells.

were expressed as percentages of the α1AT-M values obtained from the pulse-labeled cells.

Cells transfected with plasmids encoding ssCTA1 or mCTA1 were preincubated in methionine-free medium for 1 h, incubated with 0.5 ml of a 150-μCi/ml solution of [^{35}S]methionine for 1 h, and returned to serum-free medium containing 0.5 mg of methionine/ml, 20 mM HEPES (pH 7.4), and 14 mM $NaHCO_3$ for 0, 1, 2, or 3 h of chase. The preincubation and metabolic labeling were conducted at 37°C; the chase was performed at 15 or 37°C as indicated. Anti-CTA immunoprecipitations from cell extracts generated after each chase point were processed as described above, except SDS–15% PAGE was used for sample electrophoresis. Results for the chase intervals were expressed as percentages of the values obtained from the pulse-labeled cells.

RESULTS

Distribution of the CTA1 constructs. To examine the possible role of anterograde vesicular transport in the trafficking of cytosolic CTA1, we placed the coding sequence of the CTA1 polypeptide in the pcDNA3.1 eukaryotic expression vector. Three variants of this construct were made: (i) pcDNA3.1/ssCTA1 included the coding region for the CTA signal sequence immediately upstream of the CTA1 coding sequence; (ii) pcDNA3.1/ddCTA1 was identical to pcDNA3.1/ssCTA1 with the exceptions of codons that replaced glutamate with aspartate at residues 110 and 112 in the CTA1 active site, thus rendering the expressed ddCTA1 polypeptide enzymatically inactive (11); and (iii) pcDNA3.1/mCTA1 contained the active, mature CTA1 coding sequence without an upstream signal sequence. In eukaryotic cells the CTA signal sequence acts as a targeting motif for cotranslational insertion of CTA1 into the ER, and it is proteolytically removed in the ER lumen to generate the mature form of the CTA1 polypeptide (33, 38). Our investigators have previously used biochemical methods to confirm that the CTA signal sequence directs the entire pool of newly synthesized CTA1 into the ER lumen (38). Thus, newly synthesized ssCTA1 and ddCTA1 will be directed into the ER, while newly synthesized mCTA1 will be present in the cytosol.

The predicted distributions of ddCTA1, ssCTA1, and mCTA1 were confirmed by indirect immunofluorescence microscopy (Fig. 1). We found that ddCTA1 and ssCTA1 produced branching, tubularized staining patterns that colocalized with the endogenous ER chaperone PDI (Fig. 1A to D). The ssCTA1 staining pattern was more vesicular in nature than the ddCTA1 staining pattern, which may reflect different cellular responses to the presence of active versus inactive CTA1. Labeling of the nuclear envelope, which is physically contiguous with the ER (Fig. 1A and C) was clearly visible in both the ddCTA1 and ssCTA1 staining patterns. mCTA1 did not colocalize with PDI but instead produced a diffuse and unstructured staining pattern that included labeling of both the cytosol and the nucleus (Fig. 1E and F). As proteins smaller than 60 kDa can pass through the nuclear pore complex, it was not surprising that the 21-kDa mCTA1 polypeptide appeared to be present in both the cytoplasm and the nucleoplasm (Fig. 1E). Our results indicated that ddCTA1 and ssCTA1 were located in the ER, whereas mCTA1 was distributed throughout the cytoplasm and likely the nucleoplasm as well.

Most of the cells transfected with pcDNA3.1/ssCTA1 or pcDNA3.1/mCTA1 exhibited an elongated and bipolar morphology (Fig. 1C) that made it difficult to resolve the structure of the ER. The morphology of the cells presented in Fig. 1C to F is thus atypical for the populations of transfected cells expressing ssCTA1 or mCTA1. These atypical cells produced weak CTA1 immunofluorescent signals but were chosen for presentation in order to clearly visualize the structure of the ER. Very few cells expressing ddCTA1 produced the altered cell shape commonly seen in cells expressing ssCTA1 or mCTA1. Since CHO cells exhibit an elongated and bipolar morphology after exposure to exogenously added CT (8), these results indicated that ssCTA1 and mCTA1, but not ddCTA1, were enzymatically active in transfected CHO cells. It is likely that the few cells with weak CTA1 immunofluorescent signals and normal cellular morphologies did not express a sufficiently high amount of CTA1 (and cAMP) to trigger the all-or-nothing morphological response to CTA1.

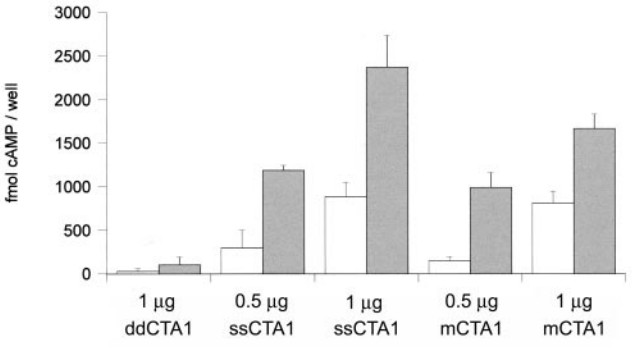

FIG. 2. In vivo activity of ddCTA1, ssCTA1, and mCTA1. CHO cells seeded to 75% confluency in six-well plates were exposed to a mixture of plasmid DNA and Lipofectamine for 3 h and were then chased for 2 h (white bars) or 4 h (gray bars). Plasmid DNA consisted of 1 μg of pcDNA3.1 (empty vector), 1 μg of pcDNA3.1/ddCTA1, 0.5 or 1 μg of pcDNA3.1/ssCTA1, or 0.5 or 1 μg of pcDNA3.1/mCTA1. Cell extracts generated at the end of the chase were assayed for cAMP content in a [^{125}I]cAMP competition assay. Background or endogenous levels of cAMP from cells transfected with the empty vector (800 to 1,000 fmol of cAMP/well) were subtracted from the other results. Data are presented as averages ± standard errors of the means of four independent experiments with duplicate samples.

Enzymatic activity of the CTA1 constructs. To further assess the cytotoxic activities of our CTA1 constructs, a [^{125}I]cAMP competition assay was used to measure cAMP levels in cells transfected with 1 μg of the empty parent vector, 1 μg of pcDNA3.1/ddCTA1, 0.5 or 1 μg of pcDNA3.1/ssCTA1, and 0.5 or 1 μg of pcDNA3.1/mCTA1 (Fig. 2). Transfection consisted of a 3-h incubation with a mixture of plasmid DNA and Lipofectamine. Intracellular cAMP levels were then quantitated at 2 and 4 h of posttransfection chase. Cells transfected with either pcDNA3.1/ssCTA1 or pcDNA3.1/mCTA1 produced significantly more cAMP than cells transfected with the empty parent vector. In contrast, cells transfected with pcDNA3.1/ddCTA1 did not produce much more cAMP than cells transfected with the empty parent vector. The extent of the cAMP response from cells transfected with either pcDNA3.1/ssCTA1 or pcDNA3.1/mCTA1 was dependent upon both the initial plasmid concentration and the time of posttransfection chase. We also found that a 16-h chase with pcDNA3.1/ssCTA1- or pcDNA3.1/mCTA1-transfected cells resulted in two- to four-fold-higher levels of intracellular cAMP than observed after 4 h of chase (data not shown), indicating that the cAMP response of transfected cells was not yet maximal after just 4 h of

chase. In addition, untransfected cells exposed to 10 ng of exogenously added CT produced more cAMP than cells transfected with either pcDNA3.1/ssCTA1 or pcDNA3.1/mCTA1 (see Fig. 4, below). This result further indicated that our system had not reached saturation at 4 h of posttransfection chase.

Drug effects on vesicular traffic and CTA1 activity. To determine whether anterograde vesicular trafficking was required for the in vivo activity of CTA1, we repeated our transfection-cAMP assay with cells exposed to caffeine, monensin, ilimaquinone (IQ), or brefeldin A (BfA)—four drugs that inhibit anterograde transport at various stages of the secretory pathway. Caffeine inhibits post-Golgi secretory traffic by an undefined, temperature-dependent mechanism (14); monensin is a carboxylic ionophore that disrupts transport in the Golgi apparatus (37); IQ prevents the formation of transport vesicles from the Golgi membrane and blocks secretory traffic at a site between the ER and medial Golgi (36); and BfA blocks vesicular transport from the ER and induces the assimilation of the Golgi apparatus into the ER (13). Drug effects on the cytotoxic activity of exogenously applied CT were also assessed.

The impacts of caffeine, monensin, IQ, and BfA on anterograde transport were initially confirmed by monitoring the drug-induced inhibition of α1AT-M secretion. α1AT-M is a soluble glycoprotein that is secreted with a $t_{1/2}$ of ~60 min (23). CHO cells transiently transfected with an α1AT-M expression plasmid were metabolically labeled for 30 min and then chased for 0 or 90 min. The amount of α1AT-M immunoprecipitated from the extracellular medium at 90 min of chase was then divided by the amount of α1AT-M immunoprecipitated from the cell extracts at 0 min of chase to determine the extent of α1AT-M secretion. Following published methodologies (references 13, 14, 36, and 37 and references therein), drug treatments were initiated during the preincubation (10 mM caffeine), metabolic labeling (10 μM IQ and 1 μg BfA/ml), or chase (10 μM monensin). The differential timing of inhibitor addition reflects the time course required for optimum drug effects. Untreated CHO cells released 94% of pulse-labeled α1AT-M after 90 min of chase, but over the same time period caffeine-treated cells only released 44% of pulse-labeled α1AT-M; monensin-treated cells released 22% of pulse-labeled α1AT-M; IQ treated cells released 16% of pulse-labeled α1AT-M; and BfA-treated cells released 1% of pulse-labeled α1AT-M (Fig. 3). The higher apparent molecular mass of the chase samples, in comparison to the pulse samples, was due to the addition of N-linked oligosaccharides to α1AT-M during transit through the Golgi apparatus. Exposure to caffeine, monensin, IQ, or BfA thus led to a significant inhibition of secretory transport.

An inhibition of cAMP production in cells transfected with pcDNA3.1/ssCTA1 or pcDNA3.1/mCTA1 and subjected to drug-induced blocks of secretory transport would indicate a requirement for anterograde trafficking for the intracellular activity of CTA1. In contrast, our results showed that drug-induced blocks to secretory transport did not affect the cAMP response of cells transfected with either pcDNA3.1/ssCTA1 or pcDNA3.1/mCTA1 (Fig. 4).

Cells transfected with pcDNA3.1/ssCTA1 or pcDNA3.1/mCTA1 and treated with caffeine produced a stronger cAMP response than the untreated, transfected control cells (Fig. 4A). Cells incubated with 10 mM caffeine throughout the posttransfection chase produced 152% (ssCTA1) or 138% (mCTA1) of the cAMP response recorded for the control cells. Caffeine-induced sensitization to CTA1 was also observed in cells exposed to exogenously added CT: cells exposed to both CT and caffeine produced 161% of the cAMP response recorded for cells exposed to just CT. Sensitization was likely due to the inhibitory action of caffeine on cAMP phosphodiesterase activity. Note, however, that a stimulatory effect arising from caffeine's action as a cAMP phosphodiesterase inhibitor would only be observed if the caffeine-induced inhibition of secretory transport did not prevent the interaction between CTA1 and Gsα. Efficient post-Golgi vesicular transport was therefore unnecessary for the in vivo activity of CTA1.

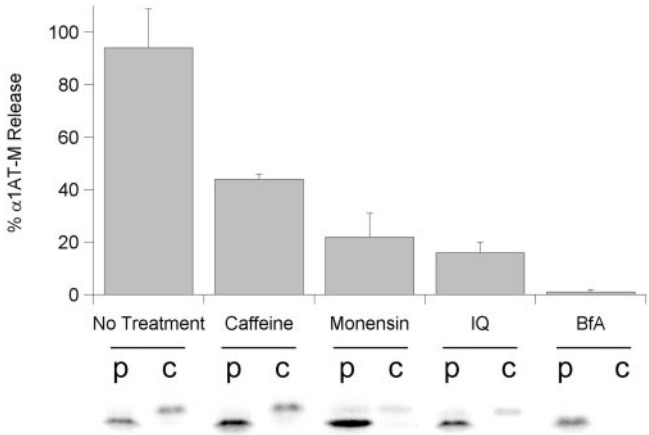

FIG. 3. Effect of caffeine, monensin, IQ, and BfA on the secretion of α1AT-M. Transfected CHO cells were preincubated in methionine-free medium for 1 h, labeled with 40 μCi of [^{35}S]methionine for 30 min, and chased in serum-free medium containing 0.5 mg of methionine/ml for 0 or 90 min. Drug treatments were initiated during the preincubation (10 mM caffeine), metabolic labeling (10 μM IQ and 1 μg BfA/ml), or chase (10 μM monensin). Immunoprecipitates from the pulse-labeled cell extracts (p) and extracellular medium after 90 min of chase (c) were visualized and quantitated by SDS-PAGE with PhosphorImager analysis. One of three independent experiments is presented in the gel; the graph represents the averages ± standard errors of the means of all three experiments.

Cells transfected with pcDNA3.1/ssCTA1 or pcDNA3.1/mCTA1 and treated with monensin generated a cAMP response similar to that observed in the untreated, transfected control cells (Fig. 4B). Cells treated with 10 μM monensin produced 120% (ssCTA1) or 108% (mCTA1) of the cAMP response recorded for the control cells. Monensin treatment resulted in a slightly greater level of sensitization to exogenously applied CT than to the transfected CTA1 constructs (149% of the untreated cAMP response to CT versus 108 to 120% of the untreated cAMP response for transfected CTA1). Sensitization to CT likely resulted from enhanced toxin trafficking from the cell surface to the ER, because the same level of sensitization was not seen when retrograde trafficking was bypassed by direct expression of CTA1 in either the ER lumen or the cytosol. Thus, monensin had a dual effect of inhibiting anterograde transport to the cell surface while enhancing retrograde transport from the cell surface to the ER. Since monensin stimulated CT activity and had no substantial effect on

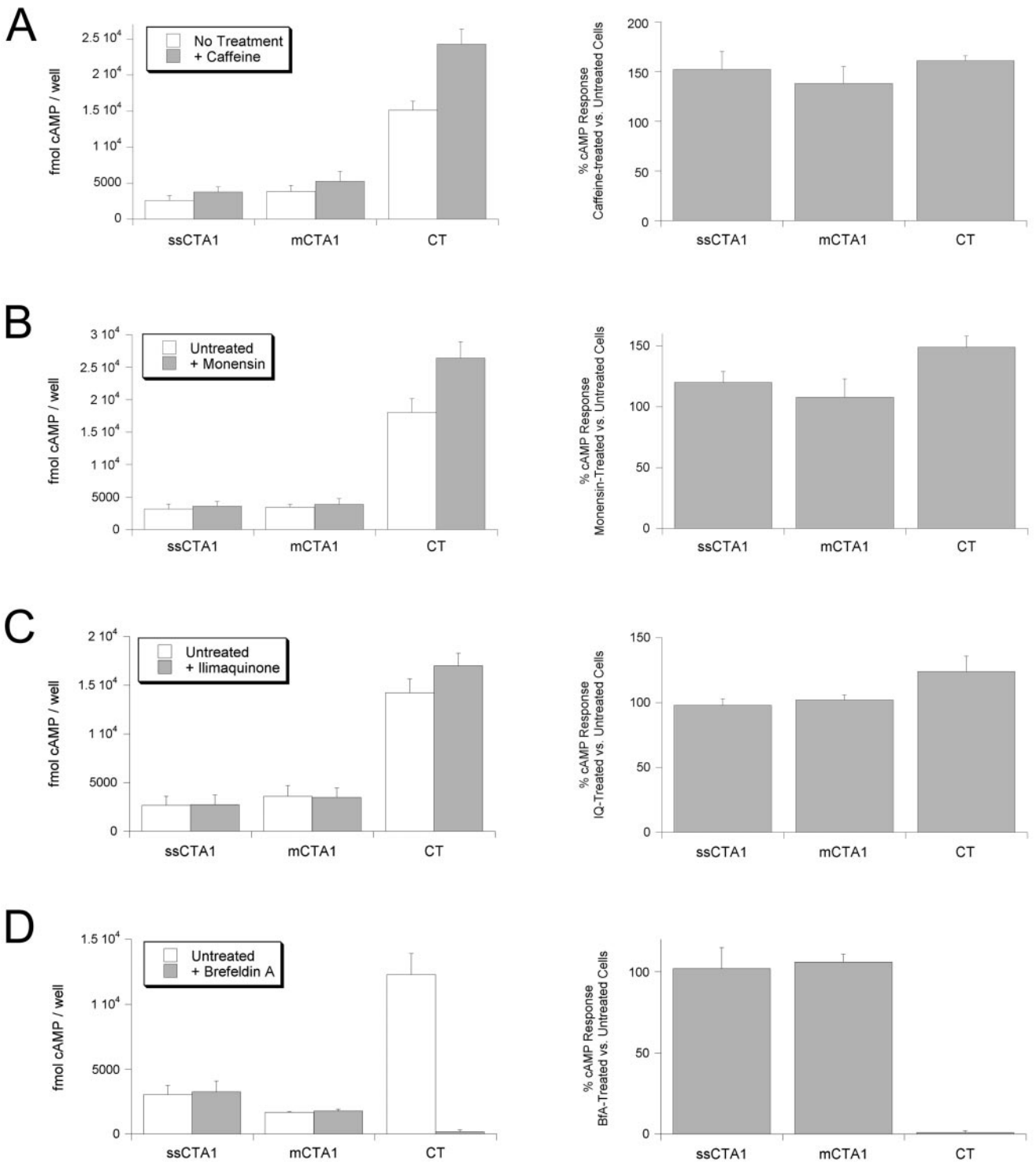

FIG. 4. Effect of caffeine, monensin, IQ, and BfA on the in vivo activity of CTA1. CHO cells exposed to a mixture of plasmid DNA and Lipofectamine for 3 h and were chased for 4 h in the absence (white bars) or presence (gray bars) of 10 mM caffeine (A), 10 μM monensin (B), 10 μM IQ (C), or 1 μg of BfA/ml (D). Plasmid DNA consisted of 1 μg of pcDNA3.1 (empty vector), 1 μg of pcDNA3.1/ssCTA1, or 1 μg of pcDNA3.1/mCTA1. In parallel experiments, untransfected CHO cells preincubated for 3 h in the absence (white bars) or presence (gray bars) of 10 mM caffeine (A), 10 μM monensin (B), 25 μM IQ (C), or 1 μg of BfA/ml (D) were subsequently exposed to 10 ng of CT/ml for 4 h in the continued presence or absence of drug. Cell extracts generated at the end of the chase were assayed for cAMP content with the use of a [^{125}I]cAMP competition assay. Background or endogenous levels of cAMP from cells transfected with an empty vector were subtracted from the other results. Data in the left panels show cAMP responses and are presented as averages ± standard errors of the means (SEMs) of at least four independent experiments with duplicate samples. Data in the right panels show the cAMP responses (averages ± SEMs) in drug-treated cells as percentages of the responses in untreated cells.

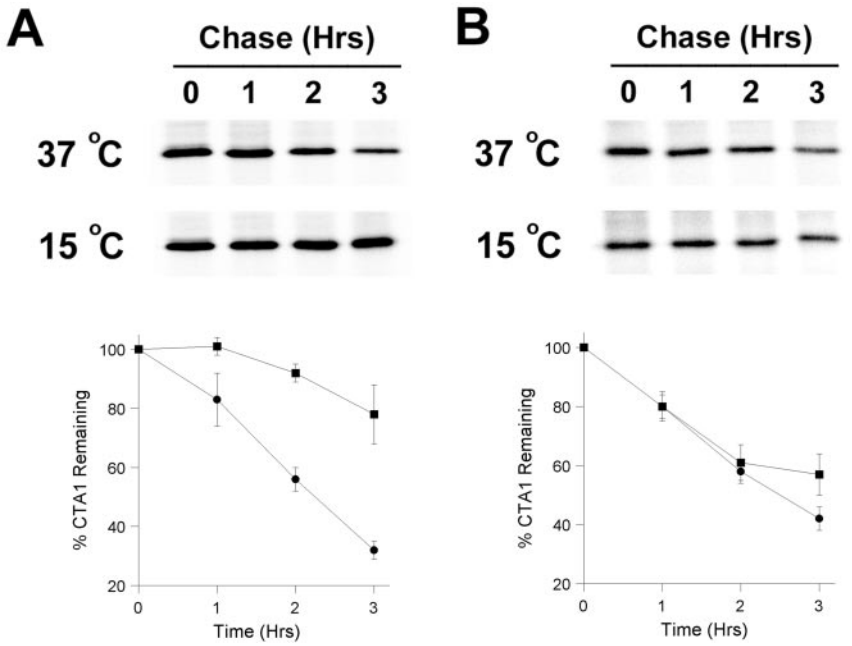

FIG. 5. Temperature-dependent degradation of ssCTA1 and mCTA1. CHO cells transfected with pcDNA3.1/ssCTA1 (A) or pcDNA3.1/mCTA1 (B) were preincubated for 1 h at 37°C in methionine-free medium and then exposed to 0.5 ml of a 150-μCi/ml solution of [^{35}S]methionine for an additional hour at 37°C. Labeled cells were chased at 15°C (squares) or 37°C (circles) in serum-free medium containing 0.5 mg of methionine/ml, 20 mM HEPES (pH 7.4), and 14 mM $NaHCO_3$. Anti-CTA immunoprecipitates from cell extracts generated at 0, 1, 2, or 3 h of chase were visualized and quantitated by SDS-PAGE with PhosphorImager analysis. One of four independent experiments is presented in the gel; the graph represents the averages ± standard errors of the means of all four experiments.

the activity of transfected CTA1, anterograde transport through the Golgi apparatus was apparently unnecessary for the in vivo activity of CTA1.

IQ treatment did not affect the cAMP response of cells transfected with either pcDNA3.1/ssCTA1 or pcDNA3.1/mCTA1 (Fig. 4C). Cells incubated with 10 μM IQ throughout the posttransfection chase generated 98% (ssCTA1) or 102% (mCTA1) of the cAMP response observed for the untreated, transfected control cells. Surprisingly, IQ treatment failed to diminish the cellular response to exogenously added CT and instead generated a mild stimulatory effect on toxicity (124% of the untreated cAMP response to CT). Previous work has shown that IQ induces a block of retrograde transport from the Golgi to the ER and therefore inhibits the cytotoxic activities of ER-translocating toxins such as ricin, *Haemophilus ducreyi* cytolethal distending toxin, *Pseudomonas aeruginosa* exotoxin A, and the Shiga-like toxins (3, 27, 36). We confirmed that IQ had an inhibitory effect on ricin intoxication of CHO cells (data not shown). CT can therefore travel from the cell surface to the ER by a retrograde transport pathway that is not inhibited by IQ. Since CT moves from the cell surface to the Golgi (6), these findings suggest that the Golgi-to-ER trafficking of CT occurs by a mechanism that is distinct from that used by ricin and the other ER-translocating toxins mentioned above.

Exposure to BfA did not inhibit the cAMP response of cells transfected with either pcDNA3.1/ssCTA1 or pcDNA3.1/mCTA1 (Fig. 4D). Cells treated with 1 μg of BfA/ml throughout the posttransfection chase produced 102% (ssCTA1) or 106% (mCTA1) of the cAMP response recorded for the untreated, transfected control cells. In separate experiments, 1 μg of BfA/ml was present during the transfection and was then removed or kept for the duration of the chase. This protocol lowered the extent of the cAMP response in all transfected cells (most likely due to a lower transfection efficiency in the presence of BfA) but did not produce any substantial differences between cells chased in the absence or presence of BfA. The inhibitory effect of BfA on exogenously applied CT confirmed the efficacy of our BfA treatment. An intact Golgi apparatus and functioning secretory pathway were therefore unnecessary for the in vivo activity of CTA1.

Temperature-dependent degradation of CTA1 constructs. The cAMP response elicited by ssCTA1 and mCTA1 in drug-treated cells indicated that anterograde secretory transport was not required for CTA1 activity. This result seemed to conflict with the observation that a 15°C incubation will block both anterograde vesicular trafficking and the in vivo activity of the free CTA1 polypeptide (17, 18, 32). However, it was possible that the 15°C block of CTA1 activity did not result from an inhibition of vesicular transport but was instead due to the inhibition of CTA1 export from the ER to the cytosol. We were unable to test this possibility with our transfection-cAMP assay because the synthesis of ssCTA1 and mCTA1 was severely inhibited at 15°C. Instead, as an alternative approach to examine whether CTA1 export from the ER to the cytosol was blocked at 15°C, we determined the half-lives of ssCTA1 and mCTA1 in cells incubated at either 15 or 37°C (Fig. 5). An inhibition of protein export from the ER to the cytosol would extend the half-life of ssCTA1, but not mCTA1, since proteosomal activity in the cytosol is required for the efficient degradation of CTA1 (38).

CHO cells transiently transfected with pcDNA3.1/ssCTA1 or pcDNA3.1/mCTA1 were metabolically labeled at 37°C and chased for 0, 1, 2, or 3 h at either 15 or 37°C. Cell extracts generated after each chase point were subjected to anti-CTA immunoprecipitation, and the immuno-isolated samples were subsequently visualized and quantitated by SDS-PAGE with PhosphorImager analysis. We found that, in comparison to the 37°C chase, a 15°C chase significantly inhibited the turnover of ssCTA1 (Fig. 5A) but had only a minor effect on the degradation of mCTA1 (Fig. 5B). The efficient turnover of mCTA1 at 15°C indicated that proteosome activity was not inhibited at 15°C. Thus, the block of ssCTA1 degradation at 15°C was most likely due to an inhibition of ssCTA1 export from the ER to the cytosol. The inability of CTA1 to enter the cytosol at 15°C would also account for its lack of cytotoxic activity at 15°C.

DISCUSSION

Plasmid-borne expression of CTA1 in either the ER or the cytosol of transfected cells generated elevated levels of intracellular cAMP. The ADP-ribosyltransferase activity of CTA1 was required to generate a cAMP response, as cells expressing the enzymatically inactive ddCTA1 construct did not produce much more than background levels of cAMP. However, the cAMP response to recombinant CTA1 (either ssCTA1 or mCTA1) never reached the level seen with exogenously applied CT. There are at least two reasons for this observation: (i) the exogenous addition of CT to a cell monolayer will expose the entire population of cells to toxin, whereas only a subpopulation of the cell monolayer will express CTA1 after transfection with the pcDNA3.1/CTA1 constructs; and (ii) cells transfected with the pcDNA3.1/CTA1 constructs do not express a maximal amount of CTA1 after just 4 h of posttransfection chase. These points are demonstrated in Fig. 2, which shows that the extent of cAMP production in transfected cells is dependent upon both the plasmid concentration (i.e., transfection efficiency) and the length of the posttransfection chase (i.e., time allowed for CTA1 synthesis). Thus, cell monolayers bathed in CT-containing medium will likely contain a greater level of cytosolic CTA1 and generate a greater cAMP response than cell monolayers transfected with pcDNA3.1/CTA1 constructs. Although CT intoxication produced a greater cAMP signal than CTA1 transfection, our transfection system yielded a reproducible and readily detectable cAMP response that was amenable to experimental manipulation as discussed below.

We were unable to directly compare the amount of cytosolic CTA1 in transfected versus intoxicated cells because the amount of CTA1 synthesized during 4 h of posttransfection chase was below the threshold for detection by metabolic labeling and immunoprecipitation. However, it should be noted that direct comparisons were not made between transfected and intoxicated cells in terms of the raw cAMP responses presented in the left panels of Fig. 4. Results under each condition (intoxication and transfection) were standardized internally by expressing the cAMP responses in drug-treated cells as percentages of the responses in untreated cells (right panels in Fig. 4). Only these standardized responses were used to make relative comparisons between transfected and intoxicated cells.

An emerging concept regarding CT trafficking proposes that CTB acts as a targeting vehicle for the delivery of CTA1 to the ER (1, 6, 43). With this model, CTB binding to GM1 gangliosides in lipid rafts on the plasma membrane results in movement of the bound toxin to the ER by retrograde vesicular traffic. Toxin disassembly then occurs in the ER, allowing the free CTA1 polypeptide to cross the ER membrane and enter the cytosol. This model predicts that CTA1 will be able to cross the ER membrane when delivered to the ER by a CTB-independent mechanism and that CTA1 will be enzymatically active when delivered to the ER or the cytosol by a CTB-independent mechanism. Results with our plasmid-borne CTA1 expression system were consistent with the proposal of CTB as an ER-targeting vehicle, since CTA1 expression in either the ER or the cytosol led to Gsα activation without the need for a prior interaction with CTB. Similar observations regarding toxin export from the ER to the cytosol and toxin activity in the cytosol have been made when the A chain of the AB-toxin ricin was expressed in the ER of either transfected yeast (34) or transfected tobacco cells (4) and when the catalytic S1 subunit of pertussis toxin was expressed in the ER or cytosol of transfected cultured cells (2, 41). The function of toxin B subunits as ER-targeting devices appears, therefore, to be a common theme in the intoxication process of ER-translocating toxins.

It has been proposed that the cytosolic pool of CTA1 reaches its Gsα target at the cytoplasmic face of the plasma membrane by traveling on anterograde-directed transport vesicles (9, 12, 19). To further examine this possibility, we conducted our transfection-cAMP assay on cells exposed to caffeine, monensin, IQ, or BfA—four drugs that block anterograde transport at different stages of the secretory pathway. An inhibition of CTA1 activity in cells with drug-induced blocks to secretory transport would provide supporting evidence for the role of anterograde transport in the intracellular activity of CTA1. In contrast, we found that none of the aforementioned drugs inhibited the cAMP response of cells transfected with pcDNA3.1/ssCTA1 or pcDNA3.1/mCTA1. Caffeine treatment resulted in a partial inhibition of α1AT-M secretion but did not inhibit the activity of CT, ssCTA1, or mCTA1. Likewise, the strong inhibition of α1AT-M secretion in monensin- or IQ-treated cells did not correspond to an inhibitory effect on CT, ssCTA1, or mCTA1. Finally, exposure to BfA resulted in an essentially complete inhibition of α1AT-M secretion (due to a block of anterograde transport) and CT toxicity (due to a block of retrograde transport, as previously reported in references 17, 26, and 29), but the activities of ssCTA1 and mCTA1 were unaffected by BfA treatment. The process of cholera intoxication thus requires retrograde vesicular transport of CT from the cell surface to the ER, but it does not require anterograde transport of the dissociated CTA1 polypeptide from the ER to the cell surface.

Previous work has shown that a 15°C incubation will block the in vivo activity of CTA1 polypeptides that have dissociated from the cholera holotoxin (17, 18). Since secretory transport is also blocked at 15°C (32), this observation seemed to indicate that a functional secretory pathway was required for CTA1 to reach its Gsα target at the plasma membrane. Yet the experiments presented here support an alternative interpretation, namely, that a 15°C incubation inhibits the ER-to-cytosol passage of the free CTA1 polypeptide. An inhibition of CTA1 export from the ER to the cytosol would prevent the ADP-

ribosylation of Gsα by CTA1. It would also block the cytosolic, proteosome-mediated degradation of our ER-localized ssCTA1 construct. It would not, however, affect the turnover of our mCTA1 construct that was expressed directly in the cytosol. A temperature-induced inhibition of CTA1 entry into the cytosol thus provides a consistent explanation for both the previously published data and the results of this study. Recent work has demonstrated that a 15°C incubation also prevents the movement of diphtheria toxin A chain from the endosomes to the cytosol (31).

Our transfection-cAMP assay allows the in vivo activity of CTA1 to be uncoupled from upstream CT trafficking events. Other assays to monitor in vivo CTA1 activity utilize exogenously applied holotoxin and therefore require a functional secretory pathway in order to elicit a cellular response to CT. The value of our transfection-cAMP assay was demonstrated by our ability to evaluate, directly and independently of CT trafficking events, the potential requirement of anterograde trafficking for the intracellular activity of CTA1. Furthermore, by comparing CT activity to ssCTA1/mCTA1 activity, we were able to distinguish events affecting retrograde CT trafficking in the endomembrane system from events affecting CTA1 activity in the cytosol. For example, monensin and IQ both generated slightly greater levels of sensitization to CT than to ssCTA1 or mCTA1. Because little stimulation of CTA1 activity was seen in monensin- or IQ-treated cells when retrograde CT transport was circumvented with plasmid-borne CTA1 expression, the observed sensitizations to CT likely resulted from drug-induced stimulations of retrograde trafficking to the ER. In contrast, it appears that caffeine altered CTA1 activity, but not CT trafficking, because it generated a similar level of sensitization to CT, ssCTA1, and mCTA1. In future studies it should be possible to use similar comparisons of CT activity versus ssCTA1/mCTA1 activity to resolve controversies regarding the inhibitory role(s) of cholesterol depletion on CT trafficking versus CTA1 interaction with Gsα (5). Finally, it should also be possible to use the transfection-cAMP assay to assess the in vivo activity of CTA1 mutants that are unable to assemble into holotoxins. Studies of this sort are under way and should provide additional novel information regarding the structure and function of CTA1.

ACKNOWLEDGMENTS

This work was supported in part by an NIH National Research Service Award (AI10394) to K. Teter and an NIH research grant (AI31940) to R. K. Holmes.

REFERENCES

1. **Badizadegan, K., A. A. Wolf, C. Rodighiero, M. Jobling, T. R. Hirst, R. K. Holmes, and W. I. Lencer.** 2000. Floating cholera toxin into epithelial cells: functional association with caveolae-like detergent-insoluble membrane microdomains. Int. J. Med. Microbiol. **290:**403–408.
2. **Castro, M. G., U. McNamara, and N. H. Carbonetti.** 2001. Expression, activity and cytotoxicity of pertussis toxin S1 subunit in transfected mammalian cells. Cell. Microbiol. **3:**45–54.
3. **Cortes-Bratti, X., E. Chaves-Olarte, T. Lagergard, and M. Thelestam.** 2000. Cellular internalization of cytolethal distending toxin from *Haemophilus ducreyi*. Infect. Immun. **68:**6903–6911.
4. **Di Cola, A., L. Frigerio, J. M. Lord, A. Ceriotti, and L. M. Roberts.** 2001. Ricin A chain without its partner B chain is degraded after retrotranslocation from the endoplasmic reticulum to the cytosol in plant cells. Proc. Natl. Acad. Sci. USA **98:**14726–14731.
5. **Fishman, P. H., and P. A. Orlandi.** 2003. Cholera toxin internalization and intoxication. J. Cell Sci. **116:**431–432.
6. **Fujinaga, Y., A. A. Wolf, C. Rodighiero, H. Wheeler, B. Tsai, L. Allen, M. G. Jobling, T. Rapoport, R. K. Holmes, and W. I. Lencer.** 2003. Gangliosides that associate with lipid rafts mediate transport of cholera and related toxins from the plasma membrane to endoplasmic reticulum. Mol. Biol. Cell **14:**4783–4793.
7. **Goins, B., and E. Freire.** 1985. Lipid phase separations induced by the association of cholera toxin to phospholipid membranes containing ganglioside GM1. Biochemistry **24:**1791–1797.
8. **Guerrant, R. L., L. L. Brunton, T. C. Schnaitman, L. I. Rebhun, and A. G. Gilman.** 1974. Cyclic adenosine monophosphate and alteration of Chinese hamster ovary cell morphology: a rapid, sensitive in vitro assay for the enterotoxins of *Vibrio cholerae* and *Escherichia coli*. Infect. Immun. **10:**320–327.
9. **Hirst, T. R.** 1999. Cholera toxin and *Escherichia coli* heat-labile enterotoxin, p. 104–129. *In* J. E. Alouf and J. H. Freer (ed.), The comprehensive sourcebook of bacterial protein toxins. Academic Press, San Diego, Calif.
10. **Holmes, R. K., and E. M. Twiddy.** 1983. Characterization of monoclonal antibodies that react with unique and cross-reacting determinants of cholera enterotoxin and its subunits. Infect. Immun. **42:**914–923.
11. **Jobling, M. G., and R. K. Holmes.** 2001. Biological and biochemical characterization of variant A subunits of cholera toxin constructed by site-directed mutagenesis. J. Bacteriol. **183:**4024–4032.
12. **Kahn, R. A., H. Fu, and C. R. Roy.** 2002. Cellular hijacking: a common strategy for microbial infection. Trends Biochem. Sci. **27:**308–314.
13. **Klausner, R. D., J. G. Donaldson, and J. Lippincott-Schwartz.** 1992. Brefeldin A: insights into the control of membrane traffic and organelle structure. J. Cell Biol. **116:**1071–1080.
14. **Kuismanen, E., J. Jantti, V. Makiranta, and M. Sariola.** 1992. Effect of caffeine on intracellular transport of Semliki Forest virus membrane glycoproteins. J. Cell Sci. **102:**505–513.
15. **Lencer, W. I., C. Constable, S. Moe, M. G. Jobling, H. M. Webb, S. Ruston, J. L. Madara, T. R. Hirst, and R. K. Holmes.** 1995. Targeting of cholera toxin and Escherichia coli heat labile toxin in polarized epithelia: role of COOH-terminal KDEL. J. Cell Biol. **131:**951–962.
16. **Lencer, W. I., C. Constable, S. Moe, P. A. Rufo, A. Wolf, M. G. Jobling, S. P. Ruston, J. L. Madara, R. K. Holmes, and T. R. Hirst.** 1997. Proteolytic activation of cholera toxin and *Escherichia coli* labile toxin by entry into host epithelial cells. Signal transduction by a protease-resistant toxin variant. J. Biol. Chem. **272:**15562–15568.
17. **Lencer, W. I., J. B. de Almeida, S. Moe, J. L. Stow, D. A. Ausiello, and J. L. Madara.** 1993. Entry of cholera toxin into polarized human intestinal epithelial cells. Identification of an early brefeldin A sensitive event required for A1-peptide generation. J. Clin. Investig. **92:**2941–2951.
18. **Lencer, W. I., C. Delp, M. R. Neutra, and J. L. Madara.** 1992. Mechanism of cholera toxin action on a polarized human intestinal epithelial cell line: role of vesicular traffic. J. Cell Biol. **117:**1197–1209.
19. **Lencer, W. I., T. R. Hirst, and R. K. Holmes.** 1999. Membrane traffic and the cellular uptake of cholera toxin. Biochim. Biophys. Acta **1450:**177–190.
20. **Lencer, W. I., S. Moe, P. A. Rufo, and J. L. Madara.** 1995. Transcytosis of cholera toxin subunits across model human intestinal epithelia. Proc. Natl. Acad. Sci. USA **92:**10094–10098.
21. **Lencer, W. I., and B. Tsai.** 2003. The intracellular voyage of cholera toxin: going retro. Trends Biochem. Sci. **28:**639–645.
22. **Majoul, I. V., P. I. Bastiaens, and H. D. Soling.** 1996. Transport of an external Lys-Asp-Glu-Leu (KDEL) protein from the plasma membrane to the endoplasmic reticulum: studies with cholera toxin in Vero cells. J. Cell Biol. **133:**777–789.
23. **McCracken, A. A., K. B. Kruse, and J. L. Brown.** 1989. Molecular basis for defective secretion of the Z variant of human alpha-1-proteinase inhibitor: secretion of variants having altered potential for salt bridge formation between amino acids 290 and 342. Mol. Cell. Biol. **9:**1406–1414.
24. **Morinaga, N., Y. Kaihou, N. Vitale, J. Moss, and M. Noda.** 2001. Involvement of ADP-ribosylation factor 1 in cholera toxin-induced morphological changes of Chinese hamster ovary cells. J. Biol. Chem. **276:**22838–22843.
25. **Moss, J., and M. Vaughan.** 1995. Structure and function of ARF proteins: activators of cholera toxin and critical components of intracellular vesicular transport processes. J. Biol. Chem. **270:**12327–12330.
26. **Nambiar, M. P., T. Oda, C. Chen, Y. Kuwazuru, and H. C. Wu.** 1993. Involvement of the Golgi region in the intracellular trafficking of cholera toxin. J. Cell Physiol. **154:**222–228.
27. **Nambiar, M. P., and H. C. Wu.** 1995. Ilimaquinone inhibits the cytotoxicities of ricin, diphtheria toxin, and other protein toxins in Vero cells. Exp. Cell Res. **219:**671–678.
28. **Orlandi, P. A.** 1997. Protein-disulfide isomerase-mediated reduction of the A subunit of cholera toxin in a human intestinal cell line. J. Biol. Chem. **272:**4591–4599.
29. **Orlandi, P. A., P. K. Curran, and P. H. Fishman.** 1993. Brefeldin A blocks the response of cultured cells to cholera toxin. Implications for intracellular trafficking in toxin action. J. Biol. Chem. **268:**12010–12016.
30. **Orlandi, P. A., and P. H. Fishman.** 1998. Filipin-dependent inhibition of cholera toxin: evidence for toxin internalization and activation through caveolae-like domains. J. Cell Biol. **141:**905–915.
31. **Ratts, R., H. Zeng, E. A. Berg, C. Blue, M. E. McComb, C. E. Costello, J. C.**

vanderSpek, and J. R. Murphy. 2003. The cytosolic entry of diphtheria toxin catalytic domain requires a host cell cytosolic translocation factor complex. J. Cell Biol. **160:**1139–1150.
32. **Saraste, J., and E. Kuismanen.** 1984. Pre- and post-Golgi vacuoles operate in the transport of Semliki Forest virus membrane glycoproteins to the cell surface. Cell **38:**535–549.
33. **Schmitz, A., H. Herrgen, A. Winkeler, and V. Herzog.** 2000. Cholera toxin is exported from microsomes by the Sec61p complex. J. Cell Biol. **148:**1203–1212.
34. **Simpson, J. C., L. M. Roberts, K. Romisch, J. Davey, D. H. Wolf, and J. M. Lord.** 1999. Ricin A chain utilises the endoplasmic reticulum-associated protein degradation pathway to enter the cytosol of yeast. FEBS Lett. **459:** 80–84.
35. **Spangler, B. D.** 1992. Structure and function of cholera toxin and the related *Escherichia coli* heat-labile enterotoxin. Microbiol. Rev. **56:**622–647.
36. **Takizawa, P. A., J. K. Yucel, B. Veit, D. J. Faulkner, T. Deerinck, G. Soto, M. Ellisman, and V. Malhotra.** 1993. Complete vesiculation of Golgi membranes and inhibition of protein transport by a novel sea sponge metabolite, ilimaquinone. Cell **73:**1079–1090.
37. **Tartakoff, A. M.** 1983. Perturbation of vesicular traffic with the carboxylic ionophore monensin. Cell **32:**1026–1028.
38. **Teter, K., R. L. Allyn, M. G. Jobling, and R. K. Holmes.** 2002. Transfer of the cholera toxin A1 polypeptide from the endoplasmic reticulum to the cytosol is a rapid process facilitated by the endoplasmic reticulum-associated degradation pathway. Infect. Immun. **70:**6166–6171.
39. **Teter, K., M. G. Jobling, and R. K. Holmes.** 2003. A class of mutant CHO cells resistant to cholera toxin rapidly degrades the catalytic polypeptide of cholera toxin and exhibits increased endoplasmic reticulum-associated degradation. Traffic **4:**232–242.
40. **Tsai, B., C. Rodighiero, W. I. Lencer, and T. A. Rapoport.** 2001. Protein disulfide isomerase acts as a redox-dependent chaperone to unfold cholera toxin. Cell **104:**937–948.
41. **Veithen, A., D. Raze, and C. Locht.** 2000. Intracellular trafficking and membrane translocation of pertussis toxin into host cells. Int. J. Med. Microbiol. **290:**409–413.
42. **Watkins, P. A., J. Moss, and M. Vaughan.** 1981. ADP ribosylation of membrane proteins from human fibroblasts. Effect of prior exposure of cells to choleragen. J. Biol. Chem. **256:**4895–4899.
43. **Wolf, A. A., M. G. Jobling, S. Wimer-Mackin, M. Ferguson-Maltzman, J. L. Madara, R. K. Holmes, and W. I. Lencer.** 1998. Ganglioside structure dictates signal transduction by cholera toxin and association with caveolae-like membrane domains in polarized epithelia. J. Cell Biol. **141:**917–927.
44. **Xu, Y., and J. T. Barbieri.** 1996. Pertussis toxin-catalyzed ADP-ribosylation of Gi-2 and Gi-3 in CHO cells is modulated by inhibitors of intracellular trafficking. Infect. Immun. **64:**593–599.
45. **Xu, Y., and J. T. Barbieri.** 1995. Pertussis toxin-mediated ADP-ribosylation of target proteins in Chinese hamster ovary cells involves a vesicle trafficking mechanism. Infect. Immun. **63:**825–832.

Editor: J. D. Clements